tions," *Journal of the Physical Society of Japan*, Vol. 17, No. 1, 1962, pp. 194–203.

[11] Williams, J. C., III and Johnson, W. D., "A Note on Unsteady Boundary Layer Separation," *AIAA Journal*, Vol. 12, No. 10, Oct. 1974, pp. 1427-1429.

[12] Sears, W. R. and D. P. Telionis, "Unsteady Boundary Layer Separation," in *Fluid Dynamics of Unsteady, Three-Dimensional and Separated Flows*, edited by F. J. Marshall, Purdue Univ., Lafayette, Ind., 1972, pp. 245–305.

[13] Howarth, L., "On the Solution of the Laminar Boundary Layer Equations," *Proceedings of the Royal Society of London*, Vol. A164, 1938, pp. 547–579.

[14] Blottner, F. G., "Finite-Difference Methods of Solution of the Boundary-Layer Equations," *AIAA Journal*, Vol. 8, No. 2, Feb. 1970, pp. 193–205.

[15] Moore, F. K. and Ostrach, S., "Displacement Thickness of the Unsteady Boundary Layer," *Journal of the Aerospace Sciences*, Vol. 24, No. 1, 1957, pp. 77–78.

OCTOBER 1974 AIAA JOURNAL VOL. 12, NO. 10

Momentum Integral Method for Viscous-Inviscid Interactions with Arbitrary Wall Cooling

MICHAEL P. GEORGEFF*
Imperial College, London, England

The momentum integral method of Klineberg is extended to allow the study of two-dimensional laminar viscous-inviscid interactions over a continuous range of wall cooling ratio. By redefining the Klineberg profile quantities, it is shown that the functions appearing in the governing differential equations become, to a good approximation, independent of wall cooling ratio. A considerable simplification of the method is thus affected and flows under nonisothermal wall conditions can be studied. Experimental comparisons are made for a wide class of body shapes which show that the method provides a good description of the major features of viscous-inviscid interactions in both supersonic and hypersonic flow and is superior to other existing methods. In the light of these comparisons, some further improvements to the method are considered.

Nomenclature

a = speed of sound; also Klineberg velocity profile parameter
A = general function
b = enthalpy profile parameter, $-\partial/\partial\eta\,(S/S_w)_{\eta=0}$
B = $(a_e p_e)/(a_\infty p_\infty)$
C = constant in viscosity relationship $(\mu/\mu_\infty)/(T/T_\infty)$
$C_0 - C_6$ = coefficients of polynomial functions
C_F = skin-friction coefficient $(\mu\,\partial u/\partial y)_w/(\frac{1}{2}\rho_\infty u_\infty{}^2)$
C_H = heat-transfer coefficient $(k\,\partial T/\partial y)_w/\rho_\infty u_\infty(h_{o_e}-h_{o_w})$
E = $\dfrac{1}{\delta_i^*}\displaystyle\int_o^{\delta_i}\frac{S}{S_w}\,dY$
f = $\dfrac{1}{1+m_e}\left[m_e F + 2H - \dfrac{1+2m_e}{m_e}Z\right] - \left[F + \dfrac{Z}{m_e}\right]\dfrac{M_e}{p_e}\dfrac{dp_e}{dM_e}$
F = $H + [(1+m_e)/m_e](1+S_w E)$
h = static enthalpy; also $\dfrac{M_e}{M_\infty}\dfrac{1+m_e}{m_e}\dfrac{Re_{\delta_{i*}}}{C}\left[\dfrac{\tan(\theta_e-\alpha_w)}{1+m_\infty} - \dfrac{\delta_i^*}{B}S_w E\dfrac{d\ln S_w}{dx}\right]$
h_o = total enthalpy
H = $\dfrac{1}{\delta_i^*}\displaystyle\int_o^{\delta_i}\frac{U}{U_e}\left(1-\frac{U}{U_e}\right)dY$
J = $\dfrac{1}{\delta_i^*}\displaystyle\int_o^{\delta_i}\frac{U}{U_e}\left(1-\frac{U^2}{U_e{}^2}\right)dY$
k = thermal conductivity
K = $M_\infty \alpha_i$
m = $[(\gamma-1)/2]M^2$
m_1, m_2 = coefficients of asymptotic expansions [Eq. (14)]
p = static pressure
$p_o, p_1, p_\alpha, p_{\alpha 1}$ = coefficients of asymptotic expansions [Eq. (13)]
P = $\delta_i^*\left[\dfrac{\partial}{\partial Y}\left(\dfrac{U}{U_e}\right)\right]_{Y=0}$
P_1 = $(P-P_B)/(1+0.25S_w)$
Pr = Prandtl number
Q = $-\delta_i^*\left[\dfrac{\partial}{\partial Y}\left(\dfrac{S}{S_w}\right)\right]_{Y=0}$
$\bar{Q}$ = $Q - \dfrac{\delta_i^* Re_{\delta_{i*}}}{BC}\dfrac{M_e}{M_\infty}T^*\dfrac{d\ln S_w}{dx}$
R = $2\delta_i^*\displaystyle\int_o^{\delta_i}\left[\frac{\partial}{\partial Y}\left(\frac{U}{U_e}\right)\right]^2 dY$
Re_x = Reynolds number, $a_\infty M_\infty x/\nu_\infty$
$Re_{\delta_{i*}}$ = Reynolds number, $a_\infty M_\infty \delta_i^*/\nu_\infty$
S = total enthalpy function, $[(h_o/h_{o_e})-1]$
T = $\displaystyle\int_o^{(\eta)_{U/U_e=0.99}}\frac{U}{U_e}\frac{S}{S_w}\,d\eta$; also static temperature
T^* = $\dfrac{1}{\delta_i^*}\displaystyle\int_o^{\delta_i}\frac{U}{U_e}\frac{S}{S_w}\,dY$
u, v = velocity components
U, V = Stewartson-Illingworth transformed velocity components
x, y = curvilinear coordinates
X, Y = Stewartson-Illingworth transformed coordinates; also Cartesian coordinates
Z = $\dfrac{1}{\delta_i^*}\displaystyle\int_o^{\delta_i}\frac{U}{U_e}\,dY$

Received November 12, 1973; revision received April 10, 1974. The author wishes to thank J. L. Stollery for his guidance and help during the course of this investigation.

Index categories: Boundary Layers and Convective Heat Transfer—Laminar; Jets, Wakes, and Viscid-Inviscid Flow Interactions; Supersonic and Hypersonic Flow.

* Department of Aeronautics; presently at the School of Education, La Trobe University, Bundoora, Victoria, Australia.

α $= \left[\int_o^{(\eta)_{U/U_e=0.99}} (1-U/U_e)\,d\eta\right]^{-1}$; also local surface slope
α_i = angle of incidence of body
γ = ratio of specific heats
δ_i = transformed boundary-layer thickness $\int_o^{(\delta_i)_{U/U_e=0.99}} dY$
δ_i^* = transformed boundary-layer displacement thickness $\int_o^{\delta_i}\left[1-\frac{U}{U_e}\right]dY$
η = Cohen-Reshotko similarity variable
θ_e = local streamline inclination at edge of boundary layer
μ = viscosity coefficient
ρ = gas density
$\tau_0-\tau_5$ = coefficients of polynomial function T
$\bar{\chi}$ = hypersonic viscous interaction parameter $M_\infty{}^3 C^{1/2}/(Re_x)^{1/2}$

Subscripts
B = Blasius values
e = local flow outside boundary layer (external)
HL = corner of flat plate-wedge (hinge line)
i = transformed (incompressible)
k, j = summation coefficients
L = characteristic length
RI = point of impingement of reflected expansion waves
SI = strong interaction
TE = trailing edge
w = wall (surface)
WI = weak interaction
∞ = freestream conditions

I. Introduction

With the advent of high altitude supersonic and hypersonic flight the analysis of laminar viscous interaction phenomena has become of considerable practical importance. Thus it is essential not only to seek a greater understanding of the structure of viscous-inviscid interactions, but also to develop workable methods capable of accurately predicting the over-all characteristics of the interaction.

At high Mach numbers, the development of the viscous layer can significantly modify the external flowfield. The usual methods of boundary-layer analysis, where viscous effects are considered as a perturbation on an already existing flow, are therefore inapplicable. However, the viscous-inviscid interaction can be described by employing the boundary-layer equations together with a "coupling" equation relating the development of the inner viscous flow to the outer inviscid flow. The governing partial differential equations can then be solved using finite-difference techniques or can be expressed in integral form and solved as ordinary differential equations.

Two of the most successful integral methods are those of Lees and Reeves[1] and Nielsen, Lynes, and Goodwin.[2] Nielsen employs a family of velocity and enthalpy profiles to provide the required relations between profile quantities and solves the first four moments of the momentum equation and the first moment of the energy equation. The method has been extended to include two-dimensional plane and axisymmetric flows with heat transfer.[3]

Lees and Reeves use the Cohen-Reshotko similarity solutions[4] to provide the required relations between boundary-layer quantities and solve the integral equations of momentum and moment of momentum together with a coupling equation based on the integral form of the continuity equation. By incorporating the energy equation Holden[5-7] and Klineberg[8] extended the method to include nonadiabatic isothermal wall conditions. The axisymmetric case was considered by Horton,[9] and by including the effects of spin, Leblanc, Horton, and Ginoux[10] further extended the method to three-dimensional adiabatic flows.

The comparisons of Murphy[11] showed that both the Klineberg and Nielsen methods provide a good description of the major characteristics of viscous-inviscid interactions at low Mach numbers. Both methods are computationally quite efficient, but a great disadvantage of the Klineberg method is that the relations between the boundary-layer profile quantities are dependent on wall cooling ratio. Additional similarity solutions must therefore be calculated at each value of wall cooling ratio in order to provide the required polynomial functions used to describe these relations. Furthermore, the method as such is incapable of describing the flow over nonisothermal surfaces.

In this paper the Klineberg profile quantities are redefined so that, to a good approximation, the profile functions become independent of wall cooling ratio. An evaluation of the method is then made by comparison with a wide range of theoretical and experimental data.

II. Analysis

A. Governing Equations

The governing equations are those of a steady two-dimensional compressible laminar boundary layer. Assuming a) the gas is calorically perfect; b) $Pr = 1$; c) $h_{o_e} = \text{const}$; and d) $\mu/\mu_\infty = C(T/T_\infty)$ where C is a constant of the Chapman-Rubesin type, and applying the Stewartson-Illingworth transformation,[12] the following integral form of these equations can be derived:

Momentum:

$$H\frac{d\ln\delta_i^*}{dx}+\frac{dH}{dx}+(2H+1+S_w E)\frac{d\ln M_e}{dx}=BC\frac{M_\infty}{M_e}\frac{P}{\delta_i^* Re_{\delta_{i*}}} \quad (1)$$

Moment of momentum:

$$J\frac{d\ln\delta_i^*}{dx}+\frac{dJ}{dx}+(3J+2S_w T^*)\frac{d\ln M_e}{dx}=BC\frac{M_\infty}{M_e}\frac{R}{\delta_i^* Re_{\delta_{i*}}} \quad (2)$$

Energy:

$$T^*\frac{d\ln\delta_i^*}{dx}+\frac{dT^*}{dx}+T^*\frac{d\ln M_e}{dx}=BC\frac{M_\infty}{M_e}\frac{Q}{\delta_i^* Re_{\delta_{i*}}}-T^*\frac{d\ln S_w}{dx} \quad (3)$$

The preceding equations are as derived by Klineberg[8] except that the total enthalpy profile quantities have been normalized with respect to the wall cooling ratio, S_w.†

The integral form of the continuity equation provides the coupling equation:

$$F\frac{d\ln\delta_i^*}{dx}+\frac{dH}{dx}+\frac{1+m_e}{m_e}S_w\frac{dE}{dx}+\frac{1}{1+m_e}\times$$
$$\left[m_e F+2H-\frac{1+2m_e}{m_e}Z\right]\frac{d\ln M_e}{dx}-\left[F+\frac{Z}{m_e}\right]\frac{d\ln p_e}{dx}=$$
$$\frac{B(1+m_e)}{m_e(1+m_\infty)}\frac{\tan(\theta_e-\alpha_w)}{\delta_i^*}-\frac{1+m_e}{m_e}S_w E\frac{d\ln S_w}{dx} \quad (4)$$

where the local static pressure p_e and streamline inclination at the edge of the boundary layer θ_e are related to the local Mach number M_e by means of the model used to describe the outer inviscid flow (see Sec. IID).

In order to solve Eqs. (1–4), the form of dependence of the profile quantities H, J, etc., on each other must be known. It is therefore assumed that the relations established for certain exact solutions are *universal* and hence valid for all flows. One then obtains a determinate set of ordinary differential equations in M_e, δ_i^*, and the parameters describing these universal relations.

B. Choice of Universal Relations

As with the method of Klineberg, the Cohen-Reshotko similarity solutions[4] are employed to provide the required universal relations between profile quantities. Two parameters are used to describe these relations, one representing the velocity profile and the other the total enthalpy profile. The velocity

† This modification to the method was first described by Georgeff[32] and independently by Gautier and Ginoux.[33] A disadvantage of the latter approach is in the use of the parameter a to describe the profile functions rather than the parameter H (see later).

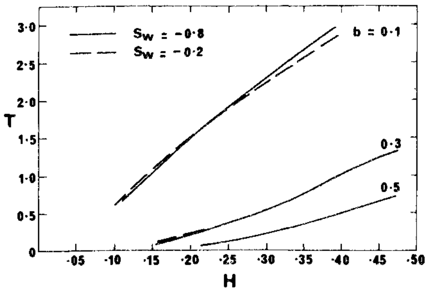

Fig. 1 Profile function $T(H, b)$.

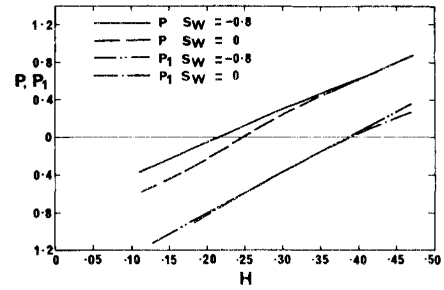

Fig. 2 Profile functions $P(H)$ and $P_1(H)$.

profile parameter is taken to be the profile quantity "H" and the total enthalpy profile parameter, normalized with respect to S_w, is taken to be

$$b = -(\partial/\partial\eta)[S/S_w]_{\eta=0} \tag{5}$$

where η is the similarity variable of Cohen and Reshotko.

Arbitrarily taking the edge of the boundary layer (η_e) at $u/u_e = 0.99$, all the profile quantities appearing in the governing differential equations can be expressed as functions of these two parameters at any particular value of S_w. The determination of the functions that depend on both the velocity and enthalpy profiles can be simplified by using the integrals

$$\alpha(H) = \left[\int_o^{\eta.99}\left(1-\frac{U}{U_e}\right)d\eta\right]^{-1}$$
$$\sigma(b) = \int_o^{\eta.99}\frac{S}{S_w}d\eta \tag{6}$$
$$T(H,b) = \int_o^{\eta.99}\frac{U}{U_e}\frac{S}{S_w}d\eta$$

such that

$$Q = b/[\alpha(H)], \quad E = \alpha(H)\sigma(b), \quad T^* = \alpha(H)T(H,b) \tag{7}$$

Whereas the enthalpy profile functions of Klineberg are strongly dependent on the wall cooling ratio, S_w (see Ref. 13), the normalized forms adopted herein are, to a good approximation, independent of S_w (see, for example, Fig. 1). Similarly, the velocity profile functions are, with the exception of $P(H)$, also very nearly independent of S_w. The dependence of $P(H)$ on S_w is not large and for practical purposes may be neglected. However, in order to retain the form of the similarity solutions, P is expressed as

$$P(H, S_w) = P_1(1+0.25S_w)+P_B \tag{8}$$

where $P_1(H)$ and P_B are taken to be independent of S_w, the subscript B denoting Blasius values. Both P and P_1 are plotted as functions of H in Fig. 2.

The advantage of using the integral quantity "H" as a parameter instead of the quantity "a" as in Klineberg's report is two-fold. First, the S_w independence of the profile functions is more accurate when these are expressed in terms of H. Second, it is not necessary to use different polynomial functions in the attached and separated flow regions as, unlike "a," the quantity H remains single valued. This implies a significant improvement in computational efficiency.

All the profile quantities appearing in this report are calculated using the data of Klineberg at $S_w = -0.8$. These quantities are then expressed as polynomial functions of the parameters H and b using a least-squares curve fit, viz,

velocity profile quantities,

$$A(H) = \sum_{k=0}^{k=6} C_k H^k$$

total enthalpy profile quantities,

$$A(b) = \sum_{k=0}^{k=5} C_k b^k$$

profile quantity "T,"

$$T(H,b) = \sum_{k=0}^{k=5} \tau_k(b)H^k$$

where

$$\tau_k(b) = \sum_{j=0}^{j=5} C_j b^j$$

The coefficients C_k, valid in the range $0.10 \leqq H \leqq 0.45$ and $0.05 \leqq b \leqq 0.55$, are given in Table 1.

Table 1 Polynomial coefficients for profile quantities

A	C_0	C_1	C_2	C_3	C_4	C_5	C_6
				Functions of parameter H			
J	$-2.69029E-02$	$3.28382E+00$	$-2.44383E+01$	$1.45692E+02$	$-4.46132E+02$	$6.96279E+02$	$-4.33666E+02$
Z	$-4.62537E-01$	$2.37071E+01$	$-2.56365E+02$	$1.58045E+03$	$-5.13908E+03$	$8.47436E+03$	$-5.44929E+03$
R	$6.27139E+00$	$-6.32363E+01$	$4.06480E+02$	$-1.65901E+03$	$4.00820E+03$	$-5.13905E+03$	$2.70259E+03$
P	$-5.99772E-01$	$8.03797E-01$	$1.54370E+01$	$-2.97149E+01$	$-2.22571E+00$	$3.78547E+01$	$0.E+00$
α	$-8.69375E-01$	$3.11317E+01$	$-3.66793E+02$	$2.25117E+03$	$-7.34057E+03$	$1.21178E+04$	$-7.86098E+03$
dJ/dH	$1.51751E+00$	$-7.94635E+00$	$7.51109E+01$	$-2.68400E+02$	$4.68822E+02$	$-3.20584E+02$	$0.E+00$
$d\alpha/dH$	$-1.21455E+01$	$4.36250E+02$	$-5.68470E+03$	$3.76888E+04$	$-1.33998E+05$	$2.42718E+05$	$-1.74007E+05$
				Functions of parameter b			
σ	$8.22871E+00$	$-6.59303E+01$	$3.10672E+02$	$-8.19937E+02$	$1.11094E+03$	$-5.98933E+02$	...
$d\sigma/db$	$-7.10897E+01$	$7.69209E+02$	$-3.82623E+03$	$9.95261E+03$	$-1.30537E+04$	$6.80598E+03$	...
τ_0	$8.65704E-01$	$-2.39401E+01$	$1.98505E+02$	$-6.81611E+02$	$1.04910E+03$	$-5.99044E+02$	...
τ_1	$1.80421E+01$	$-1.66055E+02$	$-4.51759E+02$	$4.85173E+03$	$-1.05336E+04$	$7.14417E+03$	...
τ_2	$7.04240E+01$	$-2.63002E+02$	$1.04797E+04$	$-5.87911E+04$	$1.16040E+05$	$-7.68410E+04$	...
τ_3	$-5.88181E+02$	$4.06865E+03$	$-5.85306E+04$	$2.90091E+05$	$-5.55746E+05$	$3.65010E+05$	...
τ_4	$1.47254E+03$	$-1.08777E+04$	$1.32368E+05$	$-6.34553E+05$	$1.20808E+06$	$-7.93550E+05$	...
τ_5	$-1.25964E+03$	$9.31064E+03$	$-1.07102E+05$	$5.11719E+05$	$-9.78492E+05$	$6.45847E+05$	...

C. Final Form of the Governing Differential Equations

The final form of the governing differential equations, valid for all S_w, becomes:

$$H\frac{d\ln\delta_i^*}{dx}+\frac{dH}{dx}+(2H+1+S_wE)\frac{d\ln M_e}{dx}=BC\frac{M_\infty}{M_e}\frac{P}{\delta_i^*Re_{\delta_{i*}}} \quad (9)$$

$$J\frac{d\ln\delta_i^*}{dx}+\frac{dJ}{dH}\frac{dH}{dx}+(3J+2S_wT^*)\frac{d\ln M_e}{dx}=BC\frac{M_\infty}{M_e}\frac{R}{\delta_i^*Re_{\delta_{i*}}} \quad (10)$$

$$T^*\frac{d\ln\delta_i^*}{dx}+\frac{\partial T^*}{\partial H}\frac{dH}{dx}+\frac{\partial T^*}{\partial b}\frac{db}{dx}+T^*\frac{d\ln M_e}{dx}=BC\frac{M_\infty}{M_e}\frac{\bar{Q}}{\delta_i^*Re_{\delta_{i*}}} \quad (11)$$

$$F\frac{d\ln\delta_i^*}{dx}+\frac{\partial F}{\partial H}\frac{dH}{dx}+\frac{\partial F}{\partial b}\frac{db}{dx}+f\frac{d\ln M_e}{dx}=BC\frac{M_\infty}{M_e}\frac{h}{\delta_i^*Re_{\delta_{i*}}} \quad (12)$$

The dependent variables are M_e, δ_i^*, H, and b.

D. Model for the Outer Inviscid Flow

It is necessary to choose a model for the outer inviscid flow in order to fully specify the coupling relationship [Eq. (4)]. A good model is provided by shock expansion theory. Except where shock waves interact with the boundary layer, the outer inviscid flow is assumed to be isentropic and hence the local static pressure and streamline inclination at the edge of the boundary layer can be related to the local Mach number through the Prandtl-Meyer relationship. Reference conditions are taken to be those behind the leading edge shock wave neglecting the displacement effects of the boundary layer. Hence for the flat plate at zero incidence freestream conditions are used. Such a model is strictly valid only in the very weak interaction region, but for the sake of convenience and to avoid solving the more complex equations allowing for the curvature of the leading edge shock[14] this simple model is used throughout.

Entropy changes in other regions of shock wave interaction are approximated using the model of Lees and Reeves.[1] Corner and impinging shock wave systems are equated and only the latter case is modeled. The incident shock wave is considered to impinge on the boundary layer at a point where, because of the inability of the laminar boundary layer to support a sudden rise in pressure, it is reflected as an expansion fan. The change in entropy through the shock system is thus that across the incident shock wave.

E. Boundary Conditions

It remains to specify the boundary conditions. However, unlike boundary-layer flows with prescribed pressure gradient, viscous-inviscid interactions do not form well posed initial value problems.[15] Through the mechanism of viscous interaction contained in the coupling equation, the solution is dependent on upstream and downstream boundary conditions and both must be specified.

The upstream boundary conditions are approximated by the undisturbed flat plate flow solution. For all sharp-nosed bodies the flowfield can be divided into two regions, representing the limiting cases of strong ($\bar{\chi} \gg 1$) and weak ($\bar{\chi} < 1$) interaction. Asymptotic expansions for the flow variables can be obtained in both these limits.

In the strong interaction region, the asymptotic expansions take the form

$$[p_e/p_\infty]_{SI} = p_o\bar{\chi}[1+p_\alpha K/\bar{\chi}^{1/2}+(p_1+p_{\alpha 1}K^2)/\bar{\chi}+\cdots] \quad (13)$$

where $K = M_\infty \alpha_i$ and α_i is the angle of incidence of the flat plate.

As the analytic relationship between the coefficients and S_w is quite complex, the coefficients are determined for a range of S_w and then expressed as polynomial functions in S_w using a least squares curve fit, viz,

$$A(S_w) = \sum_{k=0}^{k=3} C_k S_w^{\ k}$$

Table 2 Strong interaction asymptotic expansions

A	C_0	C_1	C_2	C_3
p_o	0.50798	0.35000	−0.01797	...
p_1	1.48735	−1.81771	−3.12003	−5.00773
p_α	1.53165	−0.01548	1.19978	...

The coefficients for $\gamma = 1.4$, valid in the range $-1 \leq S_w \leq 0$, are given in Table 2. The second-order incidence terms (i.e., those of order $K^2/\bar{\chi}$) have not been included.

In the weak interaction region the asymptotic expansions take the form

$$(M_e/M_\infty)_{WI} = 1+m_1\bar{\chi}+m_2\bar{\chi}^2+\cdots \quad (14)$$

The dependence of the coefficients on S_w is relatively simple and can be obtained directly from the governing equations. In the hypersonic limit for $\gamma = 1.4$

$$m_1 = -(0.04772+0.03453S_w)$$

and

$$m_2 = m_1^{\ 2}$$

Note that for an inclined flat plate the reference conditions in the strong interaction regime are the freestream conditions, whereas those in the weak interaction regime are the inviscid flow conditions immediately behind the leading edge shock.

In the problems under consideration, the downstream boundary condition can be of two types. If the wedge, or ramp, is very (infinitely) long, the required downstream boundary condition is that the flat plate (Blasius) solution be approached. Conversely, if the wedge is short, the downstream boundary conditions must allow for the acceleration of the flow around the trailing edge. For a sharp trailing edge a good approximation is to require that the streamwise derivatives of the flow variables (M_e, δ_i^*, H, b) become infinite at this point.[16]

F. Stability of the Governing Differential Equations

In viscous-inviscid interaction problems the governing differential equations are usually unstable to downstream integration.[15] Hence any given upstream boundary conditions will allow an infinite number of possible solutions, each of which satisfies a different downstream boundary condition. The instability of the governing differential equations thus provides the mechanism for the large scale upstream influence that is observed in many hypersonic boundary-layer flows.

However, not all of solution space exhibits this unstable behavior and in certain regions the governing differential equations are stable.[17] In these regions the solution is insensitive to downstream boundary conditions and there can be no upstream influence. In some hypersonic boundary-layer flows (e.g., expansions) this is not a physically unrealistic situation. However, if the effects of upstream influence are to be preserved (e.g., for the compression corner), it is necessary to allow a "jump" to the unstable state at the beginning of interaction.[8]

Sometimes the solution passes smoothly between regions of different stability. The transition between regions occurs at the Crocco-Lees critical point,[18] a singularity associated with the vanishing of the determinant of the governing set of equations. The critical point may be approached from the unstable region or, through changes in *local* conditions, from the stable region. In the latter case the trajectory through the critical point is not dependent on downstream conditions and there can be no upstream influence.

G. Solution Procedure

The method of solution is that used by Klineberg and is described in detail in Georgeff.[14] The upstream boundary conditions are determined and, depending on the stability of the

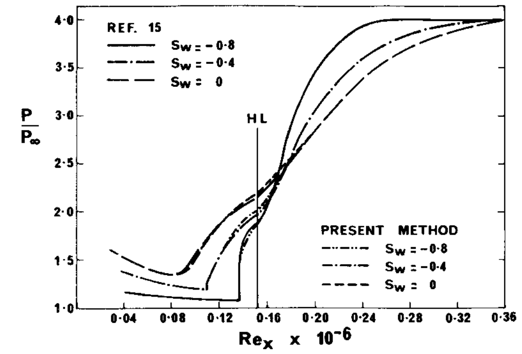

Fig. 3 Comparison of theoretical pressure distributions, $M_\infty = 6.06$, $C = 1.0$, $Re_L = 0.152 \times 10^6$.

governing differential equations and on the expected degree of upstream influence, a "jump" is or is not applied. The governing differential equations are then integrated in the downstream direction. If the resulting solution trajectory does not satisfy the downstream boundary conditions, a parameter in the upstream boundary conditions is perturbed and another solution trajectory determined. This parameter is then iterated upon until the downstream boundary conditions are satisfied.

If the Crocco-Lees critical point is encountered during integration, an extrapolation procedure is adopted to allow the solution to pass smoothly through this singularity.

Using a fourth-order Runge Kutta method to integrate the governing equations, 20–40 sec computing time on a CDC 6600 computer is required to accurately solve most viscous-inviscid interaction problems (of the order 3 sec per iteration). For a full description of the computer program, prospective users are referred to a report by Georgeff.[19]

III. Theoretical Evaluation of the S_w Normalization

Gautier and Ginoux[13] have studied the effects of wall cooling upon the characteristics of a laminar boundary-layer shock wave interaction using the method of Klineberg. They calculated additional "similar solutions" of the boundary-layer equations at discrete values of wall cooling ratio S_w in order to provide the required set of polynomial functions describing the relations between profile quantities. As no approximations were made regarding the dependence of these functions on S_w, the results provide an excellent standard of comparison for the present method.

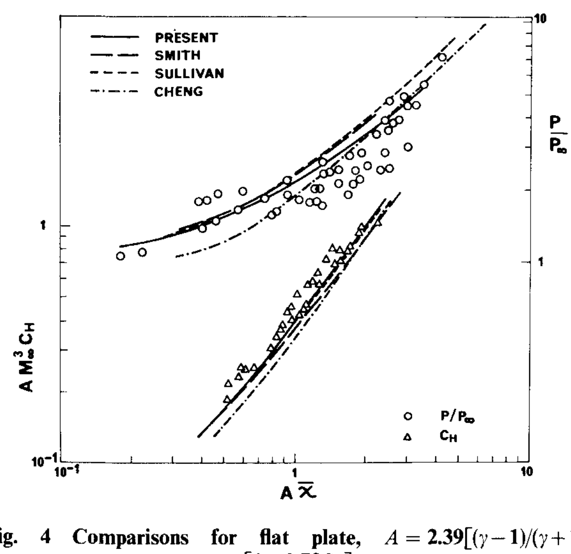

Fig. 4 Comparisons for flat plate, $A = 2.39[(\gamma-1)/(\gamma+1)] \times [1+0.72S_w]$.

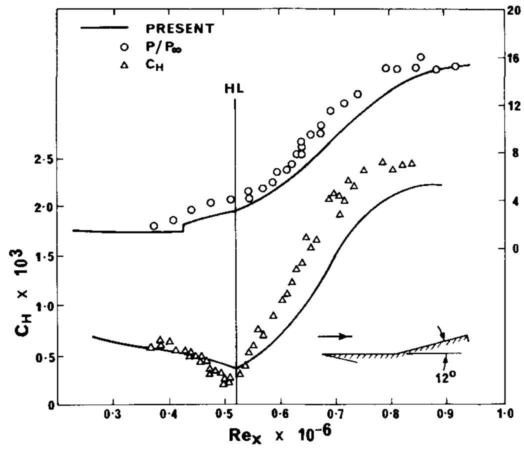

Fig. 5 Comparisons for compression corner, $M_\infty = 12.2$, $S_w = -0.78$, $C = 0.95$, $Re_L = 0.52 \times 10^6$.

The experimental conditions used are those of Lewis,[20] except that other values of wall cooling ratio are also considered. In Fig. 3, the distribution of pressure ratio obtained from the present method is compared with the results of Gautier and Ginoux at values of wall cooling ratio in the range $-0.8 \leqq S_w \leqq 0$. Both methods are seen to be in excellent agreement.

IV. Comparison with Experiment

The choice of experimental data was limited only by the requirements of two dimensionality and laminar flow. For the cases considered sufficient data is available to provide a unique solution to the analytic problem. Hence the method was used in a purely predictive capacity and no matching of theoretical and experimental results was made.

A. Sharp Flat Plate at Zero Incidence

The present momentum integral method is compared with various experimental data for the sharp flat plate at zero incidence in Fig. 4. In order to correlate the data obtained at different freestream Mach numbers and wall cooling ratios the results are expressed in the similarity form of Cheng.[21] The theoretical solution was obtained in the hypersonic limit at $S_w = -0.8$.

The predicted distributions of both pressure ratio and heat-transfer coefficient are in good agreement with the experimental data. The small overprediction of pressure ratio in the strong interaction region results from the curvature of the leading edge shock and low density effects.

Also included for comparison are the results obtained using the flat plate similarity methods of Cheng[21] and Sullivan[22] and the finite difference method of Smith.[23]

B. Compression Corner

The present method is compared with various experimental data for sharp compression corners in Figs. 5–7.

The data of Bloy[24] provides distributions of pressure ratio and heat-transfer coefficient at $M_\infty = 12.2$ and $S_w = -0.78$. The agreement between theory and experiment is seen to be very good.

The data of Holden[7] was obtained at $M_\infty = 19.8$ and $S_w = -0.95$. At the wedge angle considered, the leading edge shock interacts with the shock wave generated at the corner and the reflected expansion waves impinge on the wedge (RI in the figures), thus causing a rapid decrease in pressure ratio towards the inviscid wedge value.[25] Up to the region of impingement of the reflected expansion waves the agreement between theory and experiment is very good, especially when one considers that the entire interaction takes place in the strong

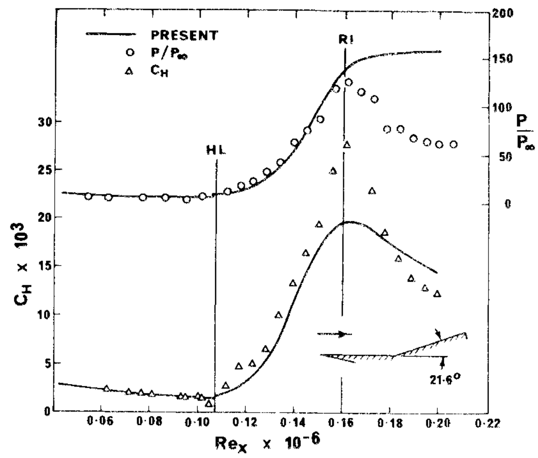

Fig. 6 Comparisons for compression corner, $M_\infty = 19.8$, $S_w = -0.95$, $C = 0.7$, $Re_L = 0.107 \times 10^6$.

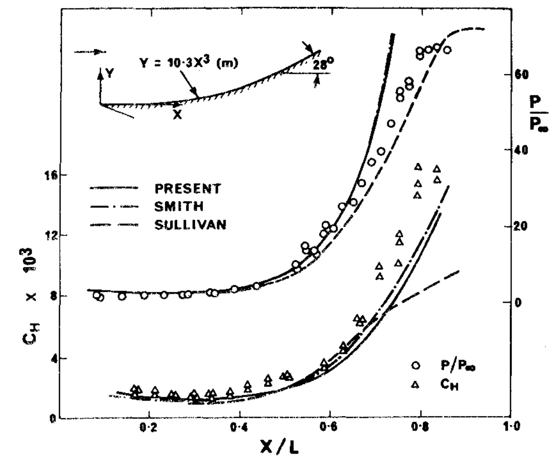

Fig. 8 Comparisons for concave surface, $M_\infty = 12.2$, $S_w = -0.78$, $C = 0.95$, $Re/m = 3.42 \times 10^6$, $L = 0.152$ m.

interaction region and that the freestream Mach number is very high. Further downstream, however, agreement cannot be expected as the model of the outer inviscid flow does not allow for reflected waves.

The data of Ball and Korkegi[26] at $M_\infty = 12.3$ and $S_w = -0.44$ represents the only data available for a wedge followed by a flap. As the flap is very short, the downstream boundary conditions for finite length wedges have been employed in determining the theoretical solution. Thus the trailing edge is seen to have some upstream influence. Note also that the pressure ratio does not reach the inviscid value over the short flap. Comparison of the theoretical results with the experimental data shows that the pressure ratio is considerably overpredicted throughout the interaction. At similar values of $\bar{\chi}_L$ and $M_\infty \alpha_w$ the data of Lewis at $S_w = 0$ and $S_w = -0.8$ (see Ref. 8) and the data of Johnson at $S_w = -0.52$ (see Ref. 14) show relatively good agreement with theory. The poor agreement with the data of Ball and Korkegi therefore appears attributable to the different configurations. The discrepancy could result in part from the reference conditions taken over the wedge, which were based on inviscid flow considerations. The effect of the viscous layer near the leading edge is to increase the shock wave angle, which would result in a reduction of pressure ratio relative to the wedge value.

In Fig. 8 comparisons are made with the data of Mohammadian[27] for flow over a concave cubic surface. The agreement between theory and experiment is good over the forward part of the surface. Far downstream the compressive disturbances coalesce to form an imbedded shock, and the resulting reflected waves cause the pressure to drop rapidly back towards the inviscid wedge value. As the flow model adopted does not allow for these reflected waves, the pressure ratio in this region is considerably overpredicted. The finite-difference method of Smith and the flat-plate similarity method of Sullivan are also included for comparison.

Other comparisons have been made at wall cooling ratios $S_w = 0$ and $S_w = -0.8$ for both sharp and rounded compression corners,[1,5-8,11,13,14,16,17,28] and in most cases the agreement with experiment is found to be very good. The only notable exceptions are the comparisons with the data of Needham.[29] Although acceptable results can be obtained using some form of matching of theoretical and experimental results,[11,13] when used in a purely predictive capacity the momentum integral method is in poor agreement with experiment. This is because the experiments of Needham were conducted in an expanding conical nozzle and lacked two-dimensionality.

C. Expansion Corner

The data of Bloy[24] for flow at Mach 12.2 over a 10° wedge followed by a sharp expansion corner is compared with theory in Fig. 9. The distributions of both pressure ratio and heat-transfer coefficient are well described by theory. The slight underprediction of pressure ratio upstream of the corner could result from the displacement effect of the boundary layer on the leading edge shock wave or from the small leading edge bluntness.

Also included for comparison are the results obtained using the method of Sullivan and the finite-difference method of Sells.[30] The solution to the Sells method was obtained using the experimentally determined pressure distribution. The good agreement between this method and the present integral method suggests that the full partial differential equations are well described using an integral approach.

In Fig. 10 comparisons are made with the data of Mohammadian[27] for flow over a convex surface. The pressure

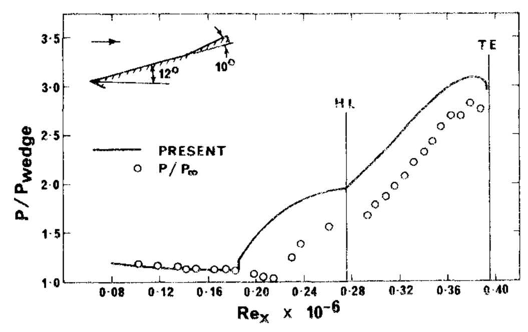

Fig. 7 Comparisons for compression corner at incidence, $M_\infty = 12.3$, $S_w = -0.44$, $C = 0.8$, $Re_L = 0.276 \times 10^6$.

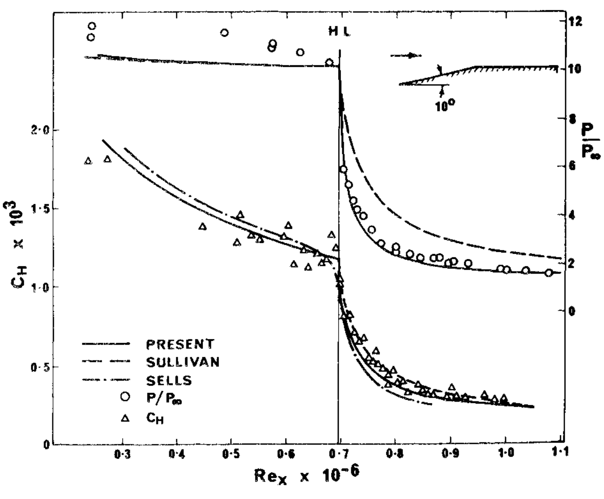

Fig. 9 Comparisons for expansion corner, $M_\infty = 12.2$, $S_w = -0.78$, $C = 0.95$, $Re_L = 0.696 \times 10^6$.

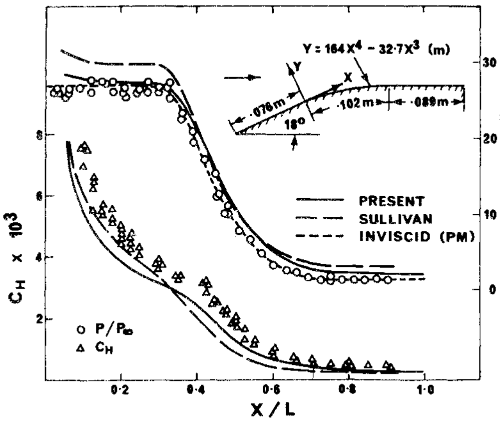

Fig. 10 Comparisons for convex surface, $M_\infty = 12.2$, $S_w = -0.78$, $C = 0.95$, $Re/m = 3.42 \times 10^6$, $L = 0.254$ m.

ratio distribution is well described by theory, but the heat-transfer coefficient is underpredicted throughout the interaction. However, comparisons with experimental data for a 20° wedge-expansion corner under identical freestream conditions show the opposite trend, with theory overpredicting the heat-transfer coefficient,[17] thus suggesting errors in the calculation of the experimental data rather than deficiencies in the momentum integral method. The results obtained using the method of Sullivan are included for comparison.

A number of other comparisons have been made for flow over sharp and curved expansion corners.[17,31] The agreement between theory and experiment is found to be very good.

D. General Comments

Although the agreement with experiment is in general very good, it is worthwhile considering whether any significant improvements to the method can be made.

The integral form of the boundary-layer equations appears adequate to describe the major characteristics of viscous-inviscid interactions. The excellent agreement between the present method and finite-difference methods suggests that in the viscous flow region the partial differential equations are well described using an integral approach.

It also appears that in most cases normal pressure gradients within the viscous layer may be neglected. Although large normal pressure gradients exist in hypersonic viscous layers, the good agreement of the predicted pressure distributions with experiment over most of the flow region suggests that their effect is small. Similarly, the related supersonic nature of the outer part of the viscous layer appears to have little effect on the solution obtained.

The model of the viscous layer thus appears adequate. However, it is clear from the comparisons that certain regions of the flow are poorly described by the present method. In these regions the model of the outer inviscid flow is seen to be inadequate. The main cause of error lies in the neglect of the reflected expansion waves resulting from strong shock interactions. In these situations the Prandtl-Meyer rule does not provide an adequate description of the flow and it may be necessary to employ the more complex method of characteristics. A small improvement in the results could be achieved by allowing for the effect of the boundary layer on the leading edge shock wave and modification of the Lees-Reeves model of shock wave boundary-layer interaction would be necessary for strong shock waves and high freestream Mach numbers.[16] Such considerations would apply to any method used in solving viscous-inviscid interaction problems.

E. Other Methods

The preceding comparisons have shown that the present momentum integral method provides better agreement with experiment than the simpler integral methods of Cheng[21] or Sullivan[22] and is comparable in accuracy to existing finite-difference methods. Furthermore, the present method is far more efficient in computational terms than finite-difference methods.

Although no comparisons between the present integral method and the integral method of Nielsen[3] have been made herein, some conclusions can be drawn from the results of earlier investigations. The comparisons of Murphy[11] showed that both methods were of comparable accuracy at low Mach numbers. However, in other experimental comparisons[2,3] the Nielsen method was shown to provide unrealistic minima in the heat-transfer rate distribution at separation and near reattachment. Thus it would appear that the present method is superior to the Nielsen method in describing separated flows.

V. Conclusions

The momentum integral method of Klineberg has been extended to allow the study of viscous interaction phenomena over a continuous range of wall cooling ratio. Suitable normalization of the boundary-layer profile quantities obviates the need to recalculate complex polynomial functions at each value of wall cooling ratio. Furthermore, flows with variable wall cooling ratio can be considered.

Comparisons made over a wide class of body shapes show that in general the agreement with experiment is good. Contrary to the conclusions reached by earlier investigators, the comparisons indicate that flows up to quite high Mach numbers are well described by the momentum integral method. In some regions, however, the agreement with experiment is found to be poor. Consideration of the outer inviscid flow suggests that these discrepancies result primarily from inadequacies in the simple model used to describe the flow properties at the edge of the boundary layer.

The comparisons also suggest that the present momentum integral method is superior to other methods in predicting the major characteristics of viscous interaction phenomena. Agreement with experiment is significantly better than obtained with the more simple integral methods of Cheng and Sullivan and the method does not show the anomalies in heat-transfer rate obtained using the integral method of Nielsen. Existing finite-difference methods do not provide significantly better agreement with experiment than the present method, and computationally are far less efficient.

References

[1] Lees, L. and Reeves, B. L., "Supersonic Separated and Reattaching Laminar Flows: I. General Theory and Application to Adiabatic Boundary Layer/Shock-Wave Interactions," *AIAA Journal*, Vol. 2, No. 11, Nov. 1964, pp. 1907–1920.

[2] Nielsen, J. N., Lynes, L. L., and Goodwin, F. K., "Calculation of Laminar Separation with Free Interaction by the Method of Integral Relations. Part I: Two-Dimensional Supersonic Adiabatic Flow. Part II: Two-Dimensional Supersonic Nonadiabatic Flow and Axisymmetric Supersonic Adiabatic and Nonadiabatic Flows," AFFDL-TR-65-107, 1965, Air Force Flight Dynamics Lab., Wright-Patterson Air Force Base, Ohio.

[3] Nielsen, J. N., Kuhn, G. D., and Goodwin, F. K., "Prediction of Supersonic Laminar Flow Separation by the Method of Integral Relations with Free Interaction," AFFDL-TR-69-87, 1970, Air Force Flight Dynamics Lab., Wright-Patterson Air Force Base, Ohio.

[4] Cohen, C. B. and Reshotko, E., "Similar Solutions for the Compressible Laminar Boundary Layer with Heat Transfer and Pressure Gradient," Rept. 1293, 1956, NACA.

[5] Holden, M. S., "An Analytical Study of Separated Flows Induced by Shock Wave-Boundary Layer Interaction," CAL Rept. AI-1972-A-3, 1965, Cornell Aeronautical Lab., Buffalo, N.Y.

[6] Holden, M. S., "Theoretical and Experimental Studies of Laminar Flow Separation on Flat Plate-Wedge Compression Surfaces in the Hypersonic Strong Interaction Regime," CAL Rept. AF-1894-A-2, 1967, Cornell Aeronautical Lab., Buffalo, N.Y.

[7] Holden, M. S., "Studies of Hypersonic Separated Flows Induced by Shock Wave-Boundary Layer Interaction," AIAA Paper 68-68, New York, 1968.

[8] Klineberg, J. M., "Theory of Laminar Viscous-Inviscid Interactions in Supersonic Flow," Ph.D. thesis, 1968, California Institute of Technology, Pasadena, Calif.; see also Klineberg, J. M. and Lees, L., "Theory of Laminar Viscous-Inviscid Interactions in Supersonic Flow," *AIAA Journal*, Vol. 7, No. 12, Dec. 1969, pp. 2211–2221.

[9] Horton, H. P., "The Calculation of Adiabatic Laminar Boundary Layer-Shock Wave Interactions in Axisymmetric Flow. Part I. Hollow Cylinder-Flare Bodies with Zero Spin," VKI TN 63, 1970, Von Kármán Institute, Brussels, Belgium.

[10] Leblanc, R., Horton, H. P., and Ginoux, J. J., "The Calculation of Adiabatic Laminar Boundary Layer-Shock Wave Interactions in Axisymmetric Flow. Part II. Hollow Cylinder-Flare Bodies with Spin," VKI TN 73, 1971, Von Kármán Institute, Brussels, Belgium.

[11] Murphy, J. D., *A Critical Evaluation of Analytic Methods for Predicting Laminar Boundary-Layer, Shock Wave Interaction*, NASA SP 228, 1969, pp. 515–539; also TN D-7044, 1971, NASA.

[12] Stewartson, K., "Correlated Compressible and Incompressible Boundary Layers," *Proceedings of the Royal Society (London)*, Vol. A200, 1949, pp. 84–100.

[13] Gautier, B. G. and Ginoux, J. J., "A Theoretical Study of Wall Cooling Effects upon Shock Wave-Laminar Boundary Layer Interaction by the Method of Lees-Reeves-Klineberg," VKI TN 71, 1971, Von Kármán Institute, Brussels, Belgium.

[14] Georgeff, M. P., "Hypersonic Laminar Boundary Layer Theory," Ph.D. thesis, 1972, Univ. of London, London, England.

[15] Garvine, R. W., "Upstream Influence in Viscous Interaction Problems," *Physics of Fluids*, Vol. 11, 1968, pp. 1413–1423.

[16] Ko, D. R. S. and Kubota, T., "Supersonic Laminar Boundary Layer Along a Two-Dimensional Adiabatic Curved Ramp," *AIAA Journal*, Vol. 7, 1969, pp. 298–304.

[17] Bloy, A. W. and Georgeff, M. P., "The Hypersonic Laminar Boundary Layer near Sharp Compression and Expansion Corners," *Journal of Fluid Mechanics*, Vol. 63, 1974, pp. 431–447.

[18] Crocco, L. and Lees, L., "A Mixing Theory for the Interaction Between Dissipative Flows and Nearly Isentropic Streams," *Journal of the Aeronautical Sciences*, Vol. 19, 1952, pp. 649–676.

[19] Georgeff, M. P., "A Computer Program for Solving Two- and Three Dimensional Laminar Viscous Interaction Problems with Arbitrary Wall Cooling Ratio," Aero. Note 73-101, 1973, Imperial College, London, England.

[20] Lewis, J. E., Kubota, T., and Lees, L., "Experimental Investigation of Supersonic Laminar Two-Dimensional Boundary Layer Separation in a Compression Corner with and without Cooling," *AIAA Journal*, Vol. 6, No. 1, Jan. 1968, pp. 7–14.

[21] Cheng, H. K., Hall, J. G., Golian, T. C., and Hertzberg, A., "Boundary-Layer Displacement and Leading-Edge Bluntness Effects in High-Temperature Hypersonic Flow," *Journal of the Aeronautical Sciences*, Vol. 28, 1961, p. 353.

[22] Sullivan, P. A., "Interaction of a Laminar Hypersonic Boundary Layer and a Corner Expansion Wave," *AIAA Journal*, Vol. 8, No. 4, April 1970, pp. 765–771.

[23] Smith, F., "The Numerical Solution of Hypersonic Laminar Boundary-Layer Problems," Ph.D. thesis, 1972, Univ. of London, London, England.

[24] Bloy, A. W., "Hypersonic Laminar Boundary-Layer Flow Over Sharp Compression and Expansion Corners," Ph.D. thesis, 1972, Univ. of London, London, England.

[25] Bird, G. A., "Effect of Wave Interactions on Pressure Distributions in Supersonic and Hypersonic Flow," *AIAA Journal*, Vol. 1, No. 3, March 1963, pp. 634–639.

[26] Ball, K. O. W. and Korkegi, R. H., "An Investigation of the Effect of Suction on Hypersonic Laminar Boundary-Layer Separation," *AIAA Journal*, Vol. 6, No. 2, Feb. 1968, pp. 239–243.

[27] Mohammadian, S., "Hypersonic Boundary Layers in Strong Pressure Gradients," Ph.D. thesis, 1970, Univ. of London, London, England.

[28] Ginoux, J. J., "Supersonic Separated Flows Over Wedges and Flares with Emphasis on a Method of Detecting Transition," VKI TN 47, 1968, Von Kármán Institute, Brussels, Belgium.

[29] Needham, D. A., "Laminar Separation in Hypersonic Flow," Ph.D. thesis, 1965, Univ. of London, London, England.

[30] Sells, C. C. L., "Two-Dimensional Laminar Compressible Boundary-Layer Programme for a Perfect Gas," ARC R & M 3533, 1966, Aeronautical Research Council, London, England.

[31] Victoria, K. J. and Kubota, T., "The Hypersonic Laminar Boundary Layer Near a Sharp Expansion Corner," AIAA Paper 70-186, New York, 1970.

[32] Georgeff, M. P., "An Extension of the Lees-Reeves-Klineberg Method to Two- and Three-Dimensional Boundary Layers with Arbitrary Wall Cooling Ratio," Aero. Rept. 72-03, 1972, Imperial College, London, England.

[33] Gautier, B. G. and Ginoux, J. J., "Improvement to Klineberg's Method for the Calculation of Viscous-Inviscid Interactions in Supersonic Flow," *AIAA Journal*, Vol. 11, No. 9, Sept. 1973, pp. 1323–1326.